EULERIAN SHAPE DESIGN OPTIMIZATION WITH FIXED GRID

Nam H. Kim[*] and Youngmin Chang[†]
Department of Mechanical & Aerospace Engineering
University of Florida
PO Box 116250
Gainesville, FL 32611-6250

ABSTRACT

Conventional shape optimization based on the finite element method uses Lagrangian representation in which the finite element mesh moves according to the shape change, while modern topology optimization uses Eulerian representation. A novel approach to shape optimization is proposed using Eulerian representation such that the mesh distortion problem in the conventional approach can be resolved. A continuum geometric model is defined on the regular, fixed grid of finite elements. An active set of finite elements that defines the discrete domain is determined using a similar procedure as the topology design. The shape design velocity field is converted into material density perturbation to calculate sensitivity information.

KEYWORDS

Shape Optimization, Topology Optimization, Boundary Homogenization, Design Sensitivity Analysis

1. INTRODUCTION

For three decades, remarkable progress has been achieved in geometry-based shape optimization.[1] Shape optimization techniques have been successfully integrated with CAD tools so that design variables are chosen from CAD parameters, providing consistency between the design and CAD models.[2] A major bottleneck of geometry-based shape optimization is the mesh distortion problem during structural analysis.[3] A regularly distributed mesh at the initial design is often distorted during shape optimization, and as a result, solution accuracy of finite element analysis deteriorates after the initial design. Although adaptive mesh-regeneration methods have been studied in order to maintain a certain level of solution accuracy, work needs to be done for these methods to be fully effective.[3] In this paper, conventional shape optimization is referred to as the Lagrangian method since both the geometry and finite element mesh move together during the shape optimization process.

In contrast to the Lagrangian method, a topology optimization method has recently been developed in order to determine the optimum structural shape without causing any mesh distortion problems.[4,5] Initial geometry of the finite element mesh maintains throughout the design process, and the material property of each element changes as a design variable. However, an excessive number of design variables make it difficult to design optimization algorithms, and results in too many local optimum solutions. In addition, the use of the optimum design often raises questions as to the feasibility of manufacturing such a design. It is non-trivial to determine structural boundary shape from topology optimization results. In contrast to the shape design, this approach is referred to as an Eulerian method since the finite element mesh is fixed during the design process.

In this paper, a new shape optimization method is proposed that uses the advantageous aspects of both conventional shape and topology optimization methods. The Lagrangian method has the advantage of accurately representing the geometric model, while the Eulerian method relieves mesh distortion problems. During structural analysis, the geometric model is placed over regularly meshed finite elements. The finite elements are fixed in the space, while the geometric model changes according to the shape design. Finite elements that belong inside the geometric model have a full magnitude of shape density, while those outside the model have a zero magnitude of shape density (a void). Finite elements on the geometric edge have a shape density that is proportional to the area fraction between the material and void. Thus, finite elements on the edge have a shape density between full material and a void. This method is similar to the homogenization method in topology optimization. Thus, in this paper it is referred to as *boundary homogenization*.

In shape optimization, a shape change in the geometric model produces a shape density change in the finite elements on the edge. As the structural shape changes, a new shape density is calculated for those elements on the edge. In addition, some elements leave the structural domain, while some enter the structural domain. Thus, accurate record keeping of each stage is an important part of the proposed approach. First, the finite elements

[*] Assistant Professor, Member AIAA
[†] Graduate Student

that belong to the boundary curve are identified by incrementally searching the boundary curve. After identifying these elements, an area fraction of each boundary element is calculated using Green's theorem. Finite elements within the structural domain can easily be identified by counting the number of boundary elements in each row or column of the grid. As opposed to Lagrangian shape representation, this approach does not require a mesh updating process. In addition, solution accuracy can be maintained throughout the design process because the same finite element size is consistently used.

One mathematical difficulty with the proposed method is to find a way to represent shape change effect as shape density change. Since shape design variables are chosen from geometric parameters, the explicit contribution of the boundary curve shape to the shape density of the boundary element is calculated based on geometric relations. Accordingly, boundary shape design velocity is related to the shape density of the boundary elements, which is used in design sensitivity calculation. Thus, the complicated shape design sensitivity formulation can be converted to a simple parametric design sensitivity formulation. In addition, numerical integration involved in the sensitivity calculation is only limited for those elements on the boundary, which provides efficiency for the proposed approach.

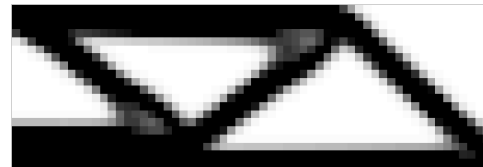## 2. EULERIAN REPRESENTATION OF GEOMETRY

Conventional geometric representation and shape optimization of a solid structure has been based on the Lagrangian approach in which the structural domain and boundary changes according to shape design parameters. Such geometric details as fillet surfaces and curvatures can be accurately represented in this approach. However, when a finite element-based numerical method is used to solve shape optimization problems, mesh distortion has been a major stumbling block for the Lagrangian approach. It is a difficult task to create a good quality mesh from complicated CAD geometry [see Figure 1(a)]. Even if a regular mesh is initially created, the mesh quality deteriorates as the structural shape changes during the design optimization. Although a number of mesh adaptation and automatic remeshing techniques have been proposed[6,7], no universal schemes have yet been developed.

Recently, many researchers[4,5] began representing a structural domain using the Eulerian approach in which the grid is fixed in space. The region occupied by material has a full shape density, while the void has zero shape density. The shape change can be characterized using a fluid flow analogy. The shape density in one region moves to neighboring regions as the structural shape changes. After being integrated with an optimiza-

tion algorithm, this approach yields the modern form of a topology design [see Figure 1(b)]. Although the topology design approach can provide a creative conceptual design, it is difficult to extract geometric information for complicated three-dimensional structures. In addition, it is complicated to physically interpret those regions with intermediate densities (a gray area) between full material and a void. However, the mesh distortion problem in the Lagrangian shape design problem can be resolved here, because mesh geometry is fixed throughout the design process.
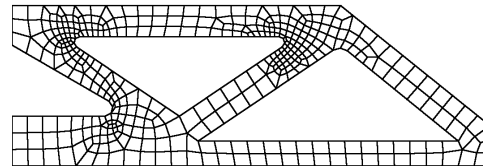
(a) Finite Element Mesh

(b) Topology Design
Figure 1. Geometric Representation Methods

As has been earlier discussed, geometry-based shape parameterization has the advantage of accurately representing the structural domain, while the Eulerian approach has the advantage of resolving the mesh distortion problem. The proposed method uses geometry-based shape parameterization on the fixed grid (see Figure 2). A solid geometry with domain Ω and boundary Γ is independently defined on a regular, rectangular mesh. If an element belongs to the domain Ω, then it has full shape density. If an element is outside domain Ω, then it has zero shape density.
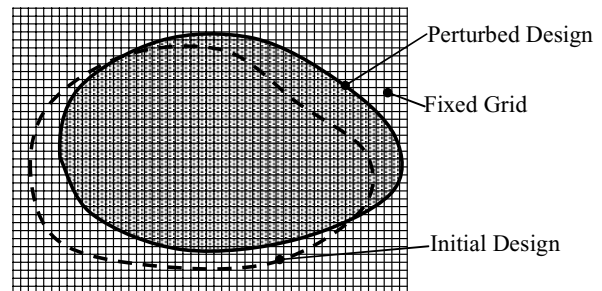

Figure 2. Design change in the fixed grid. The perturbed design occupies new regions.

American Institute of Aeronautics and Astronautics

Although the approximation in Figure 2 seems straightforward, a technical difficulty exists for those elements that reside on the structural boundary. Part of the element belongs to the structural domain, while the other part is in a void. The idea of homogenization is used for the elements on the geometric boundary. The participation of each element can be determined using *shape density*, which measures the amount of element area that belongs to the structural domain Ω. Let the area of element m be A_m, and let the area that belongs to Ω be a_m. The shape density of element m can be calculated by

$$u_m = \begin{cases} 1, & A_m \cap \Omega = A_m \\ 0, & A_m \cap \Omega = \varnothing \\ a_m / A_m, & A_m \in \Gamma \end{cases} \qquad (1)$$

where $A_m \cap \Omega = A_m$ represents the situation when element m belongs to the inside domain Ω (elements 2 and 3 in Figure 3), while $A_m \cap \Omega = \varnothing$ represents the situation when no part of element m is located in Ω (elements 7, 8, and 9). When boundary Γ resides in the element (elements 1, 4, 5, and 6), shape density u_m is the fraction of the area a_m that belongs to Ω.

7	8	9
4	5 a_5	6
1	2	3

$u_1 = 0.9$
$u_2 = 1.0$
$u_3 = 1.0$
$u_4 = 0.2$
$u_5 = 0.6$
$u_6 = 0.7$
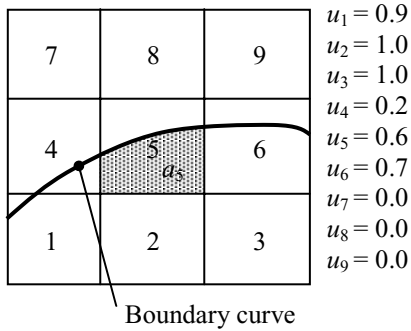$u_7 = 0.0$
$u_8 = 0.0$
$u_9 = 0.0$

Boundary curve

Figure 3. Shape densities near the geometric boundary

In order to calculate shape density u_m, domain integration is required for those elements on the geometric boundary. Since the boundary curve arbitrarily cuts through the element, it is difficult to set up a general domain integration procedure. Instead of integrating the area, Green's theorem[9] is employed to convert domain integration into boundary integration, which produces a more convenient expression. For example, for general two-dimensional problems area integration can be represented by

$$a_m = \iint_{A_m \cap \Omega} d\Omega = \int_C x_1 dx_2 \qquad (2)$$

where x_1 and x_2 are two coordinate directions, C is the curve that surrounds the area a_m, and the integration direction is counter-clockwise. Curve C consists of straight element boundary lines and a geometric boundary curve. The integral in (2) that runs along the straight

element boundary line is trivial since either x_1 or x_2 is constant. In the case of a boundary curve, it is assumed that parameter ξ is used to represent the curve, such that the expressions of $x_1(\xi)$ and $x_2(\xi)$ are available. Using the chain rule of differentiation, the integral in (2) can easily be converted to an integral with respect to parameter ξ. After calculating a_m, the shape density can be obtained from (1).

After determining the shape densities of boundary elements, the shape density of the interior or exterior can easily be determined using the following method. First, it is assumed that the geometric boundary exists within the fixed finite element grid. Starting from the left-most element in a row, the shape density value changes to either zero or one as it meets boundary elements, as illustrated in Figure 4.

Boundary elements   Boundary curve

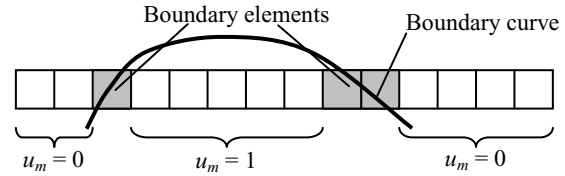$u_m = 0$ $u_m = 1$ $u_m = 0$

Figure 4. Shape densities of elements in a row

Alternatively, if the surface geometry information is available in addition to the curve geometry, than that information can be used to identify those elements that belong to interior of the geometry. For example, when a parametric surface information $\mathbf{x}(\xi, \eta)$ is available, the interior elements can be found by incrementally searching parameters ξ and η.

During structural analysis, the material property of each element is augmented using the shape density, as

$$E_m = u_m E \qquad (3)$$

where E is Young's modulus of the nominal material and E_m is the augmented modulus. Since Poisson's ratio is related to the lateral contraction during tensile deformation, it is fixed during this augmentation process. In practical application, the shape density for the void has a small value instead of zero in order to avoid numerical singularities during the finite element analysis procedure.[5]

The approximation of domain Ω in Figure 3 is different from the idea of pixel[8], in which a continuum structure is divided by a number of squares. In order to approximate the boundary reasonably, a very fine pixel mesh is required. However, with the proposed method the effect of a continuous boundary is reflected in the use of *boundary homogenization*. As an example, in Figure 5 a circle is approximated using pixel approximation and boundary homogenization. It is clear that the boundary homogenization method provides a

smooth transition between structural and void parts. Indeed, the gray boundary of the topology design result in Figure 1(b) should be understood in the same context as boundary homogenization. However, in the proposed method the structural domain is still represented using boundary curves and Figure 5(b) is a mere approximation of the geometry.
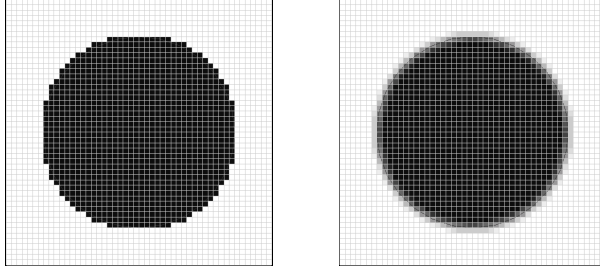
(a) Pixel approximation (b) Boundary homogenization

Figure 5. Approximation of a circle using pixel and boundary homogenization

3. FINITE ELEMENT ANALYSIS

The proposed Eulerian shape representation method has an advantage in the viewpoint of finite element analysis. Since all elements have the identical shape, it is very efficient to construct one element stiffness matrix and to use it repeatedly. Especially, when the element is square, the element stiffness matrix can be calculated analytically.[10]

In the Lagrangian approach, there exists a discrete set of nodes along the geometric boundary. Thus, displacement boundary condition can be applied to those nodes on the boundary. In the Eulerian approach since the geometry moves around within a fixed set of finite elements, it is better to apply the displacement boundary condition on the geometric curve or point. However, the geometric boundary is often located in the interior of the boundary element. Thus, it is not trivial to apply the displacement boundary condition along the geometric curve. In the regime of approximation, all elements that intersect with the displacement boundary curve are fixed during finite element analysis (see Figure 6).
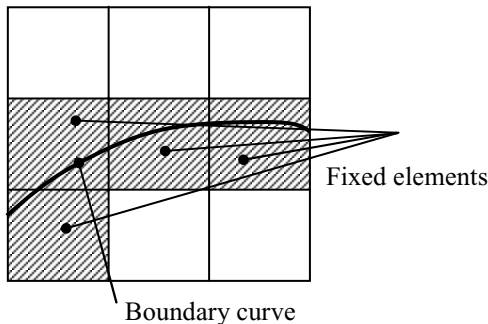

Fixed elements

Boundary curve

Figure 6. Displacement boundary conditions on the boundary elements

Even if the proposed method has many attractive features in design and simulation points of view, it requires a numerically intensive procedure due to the excessive number of finite elements in high resolution. For example, the torque arm structure in Section 6 has about 37,000 unknowns even if it is a simple, two-dimensional example. It would be very expensive to store the global stiffness matrix in the computer memory. In this paper, a sparse matrix solver in the literature[11] is employed to store only non-zero components of the global stiffness matrix and to solve the finite element matrix equations.

4. DESIGN PARAMETERIZATION

A major difference between proposed and topology design methods exists in the design parameterization process. In topology optimization, a design engineer does not have any freedom to control the design direction. The optimum shape (or topology) of the structure is determined by finding the shape density of individual elements, which does not guarantee any continuity or smoothness of the boundary. In the proposed method, design parameterization is similar to the conventional shape design problem in which the structural boundary changes according to the design velocity field. As will be shown later, it is unnecessary to define the domain design velocity field in the proposed method; the boundary design velocity field is enough to calculate design sensitivity information.

In the shape design problem, the parameters that determine the boundary curve are chosen as design variables. For example, when spline curves are used to represent the boundary, the location of control points can be chosen as design variables. As a design variable changes, the structural boundary and domain change continuously. Let the initial boundary Γ and domain Ω change to the perturbed boundary Γ_τ and domain Ω_τ, respectively. Such a shape perturbation process is analogous to the dynamic process, in which τ plays the role of time.[13] At the initial time $\tau = 0$, the structural domain is Ω and the boundary is Γ. When first-order perturbation is used, the material point $\mathbf{x}_\tau$ can be denoted by

$$\mathbf{x}_\tau = \mathbf{x} + \tau \mathbf{V}(\mathbf{x}), \quad \mathbf{x} \in \Omega \tag{4}$$

where $\mathbf{V}(\mathbf{x})$ is the design velocity field that designates the direction of shape change, and τ is a scalar parameter that controls the amount of shape change.

Equation (4) describes the shape perturbation of the continuum model. If a discrete model follows the same perturbation as (4), then it is referred to in this paper as the Lagrangian approach. As with the continuum model, the initial shape of each finite element geometry changes according to the design velocity field, which frequently results in the mesh distortion problem. However, with the Eulerian approach, the discrete finite

element model is fixed in the space (see Figure 7), and each element has a shape density value between zero and one, based on the location. The effect of shape change appears through the shape density change. Moreover, this effect only appears for those elements on the structural boundary.
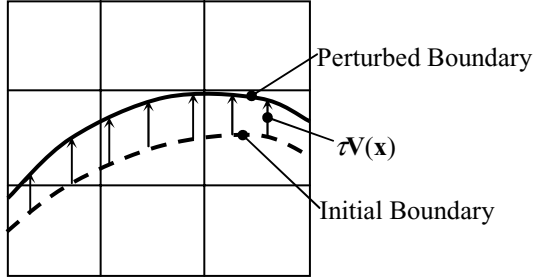

Figure 7. Shape design perturbation and corresponding change of shape density

An important theoretical issue is how to interpret shape perturbation as a shape density change on the boundary. Note that shape perturbation is given as a vector quantity (design velocity field), but that shape density variation is a scalar quantity. As the structural shape changes in the direction of the design velocity field (Figure 7), u_m of those elements on the boundary curve changes accordingly. By using standard variational formulas,[13] the change of u_m can be denoted by

$$u_{m_\tau} = u_m + \tau\, \delta u_m \tag{5}$$

where δu_m is the design variation. For those elements that reside within the structural domain, δu_m is zero. Thus, perturbation in (5) is only applied to elements on the structural boundary.

As is clear from Figure 7, when the boundary curve is perturbed in the direction of design velocity $\mathbf{V}(\mathbf{x})$, the shape density u_m also changes. Attention is focused on element m, which resides on the boundary curve. The shape density at the perturbed design can be defined as

$$u_{m_\tau} = \frac{1}{A_m}\iint_{A_m \cap \Omega_\tau} d\Omega_\tau = \frac{1}{A_m}\iint_{A_m \cap \Omega}|\mathbf{J}|\, d\Omega \tag{6}$$

where $\mathbf{J}$ is the Jacobian matrix of shape perturbation in (4), defined as

$$\mathbf{J} = \frac{\partial \mathbf{x}_\tau}{\partial \mathbf{x}} = \mathbf{I} + \tau\frac{\partial \mathbf{V}}{\partial \mathbf{x}} \tag{7}$$

The material derivative formulas for the Jacobian can be found in Choi and Haug.[13] For example, the material derivative of the Jacobian becomes

$$\frac{d}{d\tau}|\mathbf{J}|\bigg|_{\tau=0} = div\mathbf{V} \tag{8}$$

where $div\mathbf{V}$ is the divergence of the design velocity.

If the shape density in (6) is differentiated by τ, by using the formula in (8), the relation between $\mathbf{V}(\mathbf{x})$ and

δu_m can be obtained from the following relation:

$$\delta u_m = \frac{1}{A_m}\iint_{A_m \cap \Omega} div\mathbf{V}\, d\Omega = \frac{1}{A_m}\int_C \mathbf{V}^T \mathbf{n}\, d\Gamma \tag{9}$$

where $\mathbf{n}$ is the outward unit normal vector to the boundary, and C is the boundary of area a_m moving in a counter-clockwise direction. The second equality in the above equation can be obtained from the divergence theorem.[9] It is interesting and important to note that only the normal component of the boundary velocity appears in (9) because the tangential component does not contribute to the shape change.

After design parameterization is completed, the corresponding design velocity $\mathbf{V}(\mathbf{x})$ is calculated on the boundary curve. For those elements on the boundary, the variation of shape density can be calculated by integrating the design velocity along the boundary curve.

5. DESIGN SENSITIVITY ANALYSIS

The purpose of design sensitivity analysis is to develop relationships between a variation in shape and resulting variations in functionals that arise in shape design problems. For demonstration purposes, a linear elastic problem is considered in the following sensitivity development. However, a general nonlinear problem can also be taken into account using a similar approach.

In this section, design parameterization from the previous section is utilized to derive the shape sensitivity expression in terms of δu_m. The weak form[12] of the structural problem can be written in the following form:

$$a_\mathbf{u}(\mathbf{z},\overline{\mathbf{z}}) = \ell_\mathbf{u}(\overline{\mathbf{z}}), \qquad \forall \overline{\mathbf{z}} \in \mathbb{Z} \tag{10}$$

where $\mathbb{Z}$ is the space of kinematically admissible displacements, and "$\forall \overline{\mathbf{z}} \in \mathbb{Z}$" means for all virtual displacements $\overline{\mathbf{z}}$ that belong to $\mathbb{Z}$. Equation (10) is a variational equation with displacement $\mathbf{z}$ as a solution. In (10),

$$a_\mathbf{u}(\mathbf{z},\overline{\mathbf{z}}) = \iint_\Omega \boldsymbol{\varepsilon}(\overline{\mathbf{z}})^T \mathbf{C}\, \boldsymbol{\varepsilon}(\mathbf{z})\, d\Omega \tag{11}$$

and

$$\ell_\mathbf{u}(\overline{\mathbf{z}}) = \iint_\Omega \overline{\mathbf{z}}^T \mathbf{f}\, d\Omega \tag{12}$$

are the *structural bilinear* and *load linear* forms, respectively. In (11), $\boldsymbol{\varepsilon}(\mathbf{z})$ is the engineering strain vector, and $\mathbf{C}$ is the linear elastic constitutive matrix. For derivational simplicity, only body force $\mathbf{f}(\mathbf{x})$ is considered in (12). The structural problem described in (10), with definitions in (11) and (12), is a standard form in the Lagrangian approach. In this case, Ω represents the structural domain.

With the Eulerian approach, Ω is the whole domain, including both the structure and void. Let the domain Ω be composed of *NE* sub-domains (finite elements), and let each sub-domain Ω_m have shape density u_m. Then, the structural bilinear and load linear forms can be written in the following forms:

$$a_{\mathbf{u}}(\mathbf{z}, \overline{\mathbf{z}}) = \sum_{m=1}^{NE} \iint_{\Omega_m} \boldsymbol{\varepsilon}(\overline{\mathbf{z}})^T \mathbf{C} \boldsymbol{\varepsilon}(\mathbf{z}) u_m d\Omega_m \qquad (13)$$

$$\ell_{\mathbf{u}}(\overline{\mathbf{z}}) = \sum_{m=1}^{NE} \iint_{\Omega_m} \overline{\mathbf{z}}^T \mathbf{f} \, u_m d\Omega \qquad (14)$$

where in the definitions of $a_{\mathbf{u}}(\bullet,\bullet)$ and $\ell_{\mathbf{u}}(\bullet)$ the subscribed $\mathbf{u}$ is used to denote these forms' dependence on the design variable vector $\mathbf{u} = [u_1, u_2, \ldots, u_{NE}]$. Since u_m is constant within the element, it can be taken outside the integral in (13) and (14). In addition, displacement $\mathbf{z}$ in (10) implicitly depends on the design through the structural problem in (10), which must be calculated from the design sensitivity equation, as explained below.

An important component of design sensitivity analysis is calculating the variation of the state variable (in this case, displacement $\mathbf{z}$) by differentiating (10) with respect to the design, or equivalently, τ. To that end, first define the variation of the state variable, as

$$\mathbf{z}' \equiv \frac{d}{d\tau} \mathbf{z}(\mathbf{x}; \mathbf{u} + \tau \delta \mathbf{u}) \bigg|_{\tau=0} = \frac{\partial \mathbf{z}}{\partial \mathbf{u}} \bigg|_{\tau=0} \cdot \delta \mathbf{u} \qquad (15)$$

Note that $\mathbf{z}'$ depends on the design $\mathbf{u}$, where the variation is evaluated, and on the direction $\delta\mathbf{u}$ of the design variation.

Similar to (15), the structural bilinear and load linear forms can be differentiated with respect to the design. Although the design vector and its variation contain NE components, only boundary elements need to be considered in the calculation of δu_m because it is zero for those elements inside the structural domain. Let M be the number of elements that belong to the structural boundary. The variation of the structural bilinear form can be obtained using the chain rule of differentiation, as

$$\frac{d}{d\tau} a_{\mathbf{u} + \tau \delta \mathbf{u}} \left(\mathbf{z}(\mathbf{x}; \mathbf{u} + \tau \delta \mathbf{u}), \overline{\mathbf{z}} \right) \bigg|_{\tau=0} = a'_{\delta \mathbf{u}}(\mathbf{z}, \overline{\mathbf{z}}) + a_{\mathbf{u}}(\mathbf{z}', \overline{\mathbf{z}}) \quad (16)$$

where

$$a'_{\delta \mathbf{u}}(\mathbf{z}, \overline{\mathbf{z}}) = \sum_{m=1}^{M} \iint_{\Omega_m} \boldsymbol{\varepsilon}(\overline{\mathbf{z}})^T \mathbf{C} \boldsymbol{\varepsilon}(\mathbf{z}) d\Omega \, \delta u_m \qquad (17)$$

is the bilinear form's dependence on the design. If the structural problem in (10) is solved for $\mathbf{z}$ and the design variation δu_m in (9) is available as a result of design parameterization, then $a'_{\delta \mathbf{u}}(\mathbf{z}, \overline{\mathbf{z}})$ can be readily calculated following the same integration procedure used for finite element analysis. The second term on the right side of (16) is the same as the bilinear form in (13) if displacement $\mathbf{z}$ is replaced by $\mathbf{z}'$, which will be solved.

The variation of the load linear form can be obtained by following a similar procedure, as

$$\frac{d}{d\tau} \ell_{\mathbf{u} + \tau \delta \mathbf{u}}(\overline{\mathbf{z}}) \bigg|_{\tau=0} = \ell'_{\delta \mathbf{u}}(\overline{\mathbf{z}}) = \sum_{m=1}^{M} \iint_{\Omega_m} \overline{\mathbf{z}}^T \mathbf{f} \, d\Omega \, \delta u_m \qquad (18)$$

When a surface traction exists on the boundary, careful treatment is required regarding boundary homogenization, which is not developed in this paper. When a concentrated load is applied to the structure, the variation of the load linear form in (18) vanishes because the load is independent of the design.

After differentiating (10) at the perturbed design and using the formulas in (16) and (18), the following design sensitivity equation can be obtained:

$$a_{\mathbf{u}}(\mathbf{z}', \overline{\mathbf{z}}) = \ell'_{\delta \mathbf{u}}(\overline{\mathbf{z}}) - a'_{\delta \mathbf{u}}(\mathbf{z}, \overline{\mathbf{z}}), \qquad \forall \overline{\mathbf{z}} \in \mathbb{Z} \qquad (19)$$

where the solution $\mathbf{z}'$ is desired. If the right side is considered an applied load, equation (19) is similar to the structural problem in (10) with a different load, which is called the *fictitious load*. When a design variable is defined, the corresponding design velocity $\mathbf{V}(\mathbf{x})$ can be calculated on the structural boundary. Using this design velocity, the design variation δu_m can be calculated from (9).

Compared to the shape design sensitivity formulation in the Lagrangian approach, the expressions in (17) and (18) provide significantly simple computational methods, since their expressions also appear during regular finite element analysis. In geometry-based shape optimization, domain integration is involved in (17) and (18). However, only the boundary integral is sufficient for the proposed method.

6. NUMERICAL EXAMPLE

In this section, a numerical example is presented in order to compare with the shape optimization results in the literature.[3,14]

A torque arm shown in Figure 8 is composed of 32 points, 28 boundary curves, and 16 surfaces. A rectangular domain is established with lower-left corner being (-7, -8) and upper-right corner being (49, 8), which covers the whole structure. A 0.471 cm × 0.471 cm square is used to discretize the rectangular domain. Figure 8 also shows the structural domain that is identified using the boundary homogenization method. The black interior domain has a full shape density ($u = 1$), while the gray boundary represents intermediate shape density ($0 < u < 1$) calculated using (1). For material properties, the following values are use: Young's modulus = 207.4 GPa, Poisson's ration = 0.3, and thickness = 0.3 cm.

In finite element analysis, the left circle is fixed and horizontal and vertical forces are applied at the center of the right circle. In order to apply for the displacement boundary conditions, the boundary curves that correspond to the left circle are identified first. It is trivial to retrieve boundary element information corresponding to the displacement boundary curves. Then, all nodes that belong to the boundary elements are fixed. Thus, in this approach displacement boundary

conditions are applied in a layer of elements. The force boundary condition can also be applied in the same manner.
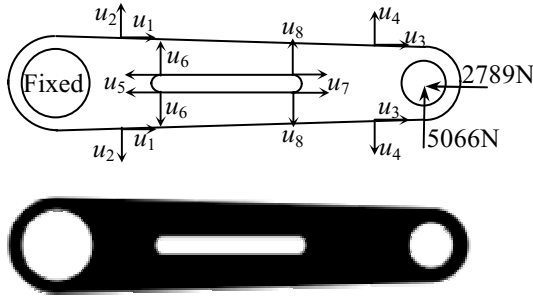

Figure 8. Design parameterization and boundary homogenization of a torque arm with pixel size=0.47cm

Maximum stress of about 361 MPa appears at the top and bottom surface of the torque arm (see Figure 9). This result is expected because the applied force is superposition of compressive and bending loads. In addition, relatively high stress concentration is observed at the end of interior slot, which is caused by distortion at the small radius region.

In the mathematical point of view, the pixel-based geometric representation may cause singularity at the non-smooth boundary, which is inevitable when inclined boundary is approximated by x- and y-directional squares. However, the proposed approach reduces such singularity by gradually reducing the shape density at the boundary. However, different material properties between interior and boundary elements cause stress discontinuity. Smoothening algorithm in stress may help to reduce discontinuity.
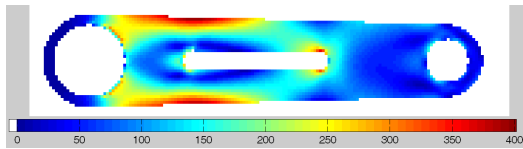

Figure 9. Finite element analysis results of the torque arm (equivalent stress plot)

Since design parameters are defined on the geometric model, the horizontal and vertical movements of geometric points can be selected as design parameters. Eight design parameters are chosen that can change the boundary of the torque arm (see Figure 8). In order to maintain symmetric geometry, design parameters are linked. As design parameters are changed, new shape density for each finite element is calculated from which the material constants are changed as depicted in (3).

A simple design optimization problem is posed to minimize the weight of the structure, while satisfying the maximum stress constraint. In order to induce large shape change, a loose constraint limit is deliberately provided. Thus, the design optimization problem can be stated that

$$\begin{cases} \text{minimize} & \text{weight} \\ \text{subject to} & \sigma_{max} \leq 800\,\text{MPa} \end{cases} \quad (20)$$

The lower and upper bounds of design parameters are selected such that the topology of structure maintains.

The design optimization problem is solved using the sequential quadratic programming method in Design Optimization Tool (DOT).[15] A function values and sensitivity information is provided to the gradient-based optimization algorithm. The design optimization problem is converged after eleven number of design iteration. Figure 10 shows the scaled history plot of objective function and constraint. The optimum design reduces more than 40% of the structural weight. The maximum stress at the optimum design appears to be 789 MPa.
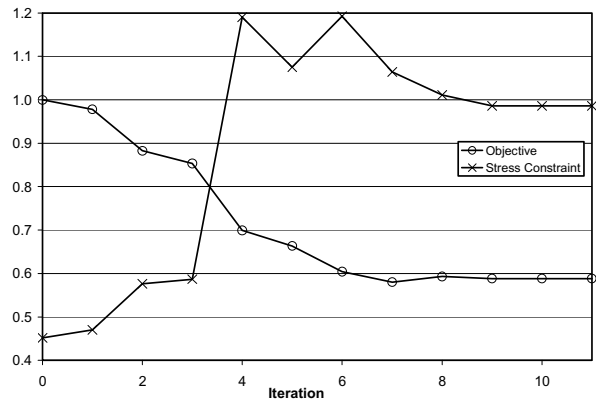

Figure 10. Design optimization histories for objective function (Weight) and constraint (maximum stress)

Figure 11 shows the stress contour plot at the optimum design. The optimization algorithm chose the geometry such that the maximum stress is evenly distributed along the upper and lower regions of the structure. The optimum design conforms to engineering sense because such a beam-like structure the moment of inertia needs to be increased as the moment arm increases.
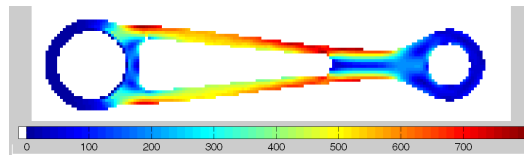

Figure 11. Finite element analysis results at the optimum design

7. CONCLUSION

A new domain approximation method using an Eulerian description is developed for the structural optimization problem. Boundary homogenization provides a unique approximation of the structural domain and boundary on the fixed grid of finite elements. Design parameterization on the geometric model provides accurate representation of design intent, and the shape density concept resolves the mesh distortion problem that exists in the Lagrangian approach. The transformation of the design velocity field into a shape density variation plays a key role in making this approach possible.

In order to be a practical engineering tool, the proposed approach needs to be extended to three-dimensional structures, which involves in boundary homogenization of a volume. As system's degrees-of-freedom increase significantly, an iterative matrix solver may need to be incorporated.

REFERENCES

1. R. T. Haftka and R. V Grandhi, Structural Shape Optimization – A Survey, Computer Methods in Applied Mechanics and Engineering, Vol. 57, No. 1, 91 – 106, 1986

2. E. Hardee, K. H. Chang, J. Tu, K. K. Choi, I. Grindeanu, X. M. Yu, A CAD-Based Design Parameterization for Shape Optimization of Elastic Solids, Advances in Engineering Software, Vol. 30, No. 3, 185 – 199, 1999

3. J. A. Bennett and M. E. Botkin, Structural Shape Optimization with Geometric Description and Adaptive Mesh Refinement, AIAA Journal, Vol. 23, No. 3, 458 – 464, 1985

4. K. Suzuki and N. Kikuchi, A Homogenization Method for Shape and Topology Optimization, Computer Methods in Applied Mechanics and Engineering, Vol. 93, No. 3, 291 – 318, 1991

5. M. P. Bendsøe, Optimization of Structural Topology, Shape, and Material, Springer-Verlag, Berlin, Heidelberg, 1995

6. R. R. Salagame and A. D. Belegundu, Distortion, degeneracy and rezoning in finite elements – a survey, Sadhana-Academy Proceedungs in Engineering Sciences, Vol. 19, 311 – 335, 1994

7. O. C. Zienkiewicz and J. Z. Zhu, Adaptivity and mesh generation, International Journal for Numerical Methods in Engineering, VOl. 32, No. 4, 783 – 810, 1991

8. K. Terada, T. Miura, and N. Kikuchi, Digital Image-Based Modeling Applied to the Homogenization Analysis of Composite Materials, Computational Mechanics, Vol. 20, No. 4, 331 – 346, 1997

9. E. J. Haug and K. K. Choi, Methods of Engineering Mathematics, Prentice-Hall, Englewood Cliffs, New Jersey, 1993

10. O. Sigmund, A 99 Line Topology Optimization Code with the Matlab, Structural and Multidisciplinary Optimization, Vol. 21, 120–127, 2001

11. K. S. Kundert, Sparse Matrix Technique. In Circuit Analysis, Simulation, and Design, Albert Ruehli ed. North-Holland, 1986

12. T. J. R. Hughes, The Finite Element Method Linear Static and Dynamic Finite Element Analysis, Prentice-Hall, Englewood Cliffs, New Jersey, 1987

13. K. K. Choi and E. J. Haug, Shape Design Sensitivity Analysis of Elastic Structures. Journal of Structural Mechanics, Vol. 11, 231 – 269, 1983

14. N. H. Kim, K. K. Choi, M. E. Botkin, Numerical Method for Shape Optimization Using Meshfree Method, Structural Multidisciplinary Optimization, in press, 2003

15. G. N. Vanderplaats, DOT User's Manual, VMA Corp., 1997